New Journal of Physics
The open-access journal for physics

Iron isotope effect on the superconducting transition temperature and the crystal structure of $FeSe_{1-x}$

R Khasanov[1,5], M Bendele[1,2], K Conder[3], H Keller[2], E Pomjakushina[2] and V Pomjakushin[4]

[1] Laboratory for Muon Spin Spectroscopy, Paul Scherrer Institute, CH-5232 Villigen PSI, Switzerland
[2] Physik-Institut der Universität Zürich, Winterthurerstrasse 190, CH-8057 Zürich, Switzerland
[3] Laboratory for Developments and Methods, Paul Scherrer Institute, CH-5232 Villigen PSI, Switzerland
[4] Laboratory for Neutron Scattering, ETH Zürich and PSI, CH-5232 Villigen PSI, Switzerland
E-mail: rustem.khasanov@psi.ch

New Journal of Physics **12** (2010) 073024 (8pp)
Received 10 May 2010
Published 22 July 2010
Online at http://www.njp.org/
doi:10.1088/1367-2630/12/7/073024

Abstract. The Fe isotope effect (Fe-IE) on the transition temperature T_c and the crystal structure was studied in the Fe chalcogenide superconductor $FeSe_{1-x}$ by means of magnetization and neutron powder diffraction (NPD). The substitution of natural Fe (containing $\simeq 92\%$ of ^{56}Fe) by its lighter ^{54}Fe isotope leads to a shift in T_c of 0.22(5) K corresponding to an Fe-IE exponent of $\alpha_{Fe} = 0.81(15)$. Simultaneously, a small structural change with isotope substitution is observed by NPD, which may contribute to the total Fe isotope shift of T_c.

Historically, the isotope effect played a crucial role in elucidating the origin of the pairing interaction leading to the occurrence of superconductivity. The discovery of the isotope effect on the superconducting transition temperature T_c in Hg [1] in 1950 provided the key experimental evidence for phonon-mediated pairing as formulated theoretically by Bardeen–Cooper–Schrieffer (BCS) theory subsequently. The observation of unusually high T_cs in the newly discovered Fe-based superconductors immediately raised the question regarding the pairing glue and initiated isotope effect studies. Currently, we are aware of two papers on isotope experiments with, however, contradicting results. Liu *et al* [2] showed that in

[5] Author to whom any correspondence should be addressed.

$SmFeAsO_{0.85}F_{0.15}$ and $Ba_{0.6}K_{0.4}Fe_2As_2$ the Fe isotope effect (Fe-IE) exponent defined as [3]

$$\alpha_{Fe} = -\mathrm{d}\ln T_c/\mathrm{d}\ln M_{Fe} = -(\Delta T_c/T_c)/(\Delta M_{Fe}/M_{Fe}) \quad (1)$$

reaches values of $\alpha_{Fe} \simeq 0.35$ (M_{Fe} is the Fe atomic mass), while Shirage *et al* [4] found a negative Fe-IE exponent $\alpha_{Fe} \simeq -0.18$ in $Ba_{1-x}K_xFe_2As_2$. Note that the only difference between the $Ba_{1-x}K_xFe_2As_2$ samples studied in [2, 4] was the preparation procedure (low-pressure synthesis in [2] versus high-pressure synthesis in [4]), while the potassium doping ($x \simeq 0.4$) as well as the T_cs for the samples containing natural Fe ($T_c \simeq 37.3$ K in [2] versus $T_c \simeq 37.8$ K in [4]) were almost the same.

In this paper, we study the Fe-IE on T_c and on the structural parameters (such as the lattice parameters a, b and c, the lattice volume V and the distance between the Se atom and Fe plane (Se height) h_{Se}) for another representative of the Fe-based high-temperature superconductors (HTS), namely $FeSe_{1-x}$ [5]–[11]. The substitution of natural Fe (containing $\simeq 92\%$ of ^{56}Fe) by its lighter ^{54}Fe isotope leads to a shift in T_c of 0.22(5) K corresponding to an Fe-IE exponent of $\alpha_{Fe} = 0.81(15)$.

The $^{54}FeSe_{1-x}/^{56}FeSe_{1-x}$ samples (hereafter we denote natural Fe containing $\simeq 92\%$ of ^{56}Fe isotope as ^{56}Fe) with the nominal composition $FeSe_{0.98}$ were prepared by a solid state reaction made in two steps. Pieces of Fe (natural Fe: 99.97% minimum purity, average atomic mass $M_{Fe} = 55.85\,\mathrm{g\,mol^{-1}}$, or ^{54}Fe: 99.99% purity, 99.84% isotope enriched, $M_{^{54}Fe} = 54.0\,\mathrm{g\,mol^{-1}}$) and Se (99.999% purity) were first sealed in double-walled quartz ampules, heated up to 1075 °C, annealed for 72 h at this temperature and 48 h at 420 °C, and then cooled down to room temperature at a rate of 100 °C $\mathrm{h^{-1}}$. As a next step, the samples, taken out of the ampules, were powderized, pressed into pellets, sealed into new ampules and annealed first at 700 °C for 48 h and then at 400 °C for 36 h, followed by cooling to room temperature at a rate of 200 °C $\mathrm{h^{-1}}$. Due to the extreme sensitivity of $FeSe_{1-x}$ to oxygen [7, 8], all the intermediate steps (grinding and pelletizing), as well as the preparation of the samples for the neutron powder diffraction (NPD) and magnetization experiments, were performed in a glove box in a He atmosphere.

The Fe-IE on the structural properties was studied by NPD experiments by using the high-resolution powder diffractometer HRPT (Paul Scherrer Institute, Switzerland) [12]. The experiments were carried out at a wavelength $\lambda = 1.494$ Å. The $^{54}FeSe_{1-x}/^{56}FeSe_{1-x}$ samples, placed into vanadium containers, were mounted into a He-4 cryostat in order to reach temperatures between 5 and 250 K. High statistics data were taken at 250 and 5 K. Data at $10 \leqslant T \leqslant 240$ K were collected with intermediate statistics.

Figure 1 shows the NPD spectra taken at $T = 250$ K. The differences in peak intensities, clearly visible at small θ, are caused by the different values of the coherent neutron scattering length (b_{coh}) of natural Fe and that of the ^{54}Fe isotope. The refinement of the crystal structure was performed by using the FULLPROF program [13] with $b_{coh}^{Fe} = 9.45 \times 10^{-15}$ m, $b_{coh}^{^{54}Fe} = 4.2 \times 10^{-15}$ m and $b_{coh}^{Se} = 7.97 \times 10^{-15}$ m [15]. The refined structural parameters at $T = 250$ and 5 K are summarized in table 1. The amount of impurity phases and the Se content $(1-x)$, determined for the data sets taken at $T = 250$ K, were kept fixed during the refinement of the NPD spectra at lower temperatures. The mass fractions of impurity phases, the hexagonal FeSe ($P6_3/mmc$) and Fe ($Im3m$) [14], were found to be 0.50(10)%, 0.31(4)% and 1.13(18)%, 1.06(7)% for $^{54}FeSe_{1-x}$ and $^{56}FeSe_{1-x}$, respectively.

Figure 2 shows the temperature dependence of the lattice parameters a, b and c, the lattice volume V and the Se height h_{Se} of a representative $^{54}FeSe_{1-x}$ and a representative $^{56}FeSe_{1-x}$

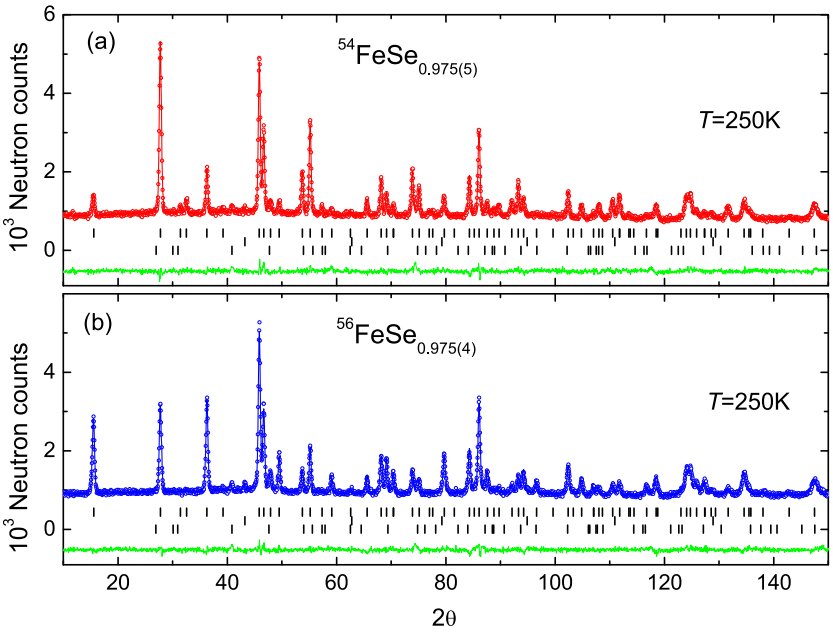

Figure 1. The Rietveld refinement pattern and difference plot of NPD data for $^{54}FeSe_{1-x}$ (panel a) and $^{56}FeSe_{1-x}$ (panel b) at $T = 250$ K. The rows of ticks show the Bragg-peak positions for the main phase FeSe ($P4nmm$) and two impurity phases: Fe ($Im3m$) and hexagonal FeSe ($P6_3/mmc$). The main tetragonal phase corresponds to 0.975(5) and 0.975(4) Se occupancy for $^{54}FeSe_{1-x}$ and $^{56}FeSe_{1-x}$, respectively.

sample (see figure 3). From figure 2(a), it is obvious that at $T_s \simeq 100$ K a transition from a tetragonal to an orthorhombic structure takes place, analogous to that reported in [7, 9, 16]. The Fe-IE on the structural transition temperature T_s could be estimated from the shift of the interception point of the linear fits to $a(T)$ and $b(T)$ in the vicinity of T_s, as denoted by the arrows in the inset of figure 2(a), which was found to be $\Delta T_s = 0.2(2.5)$ K. Within the whole temperature range ($5\,\text{K} \leqslant T \leqslant 250\,\text{K}$), the lattice constants a and b are slightly larger for $^{54}FeSe_{1-x}$ than those for $^{56}FeSe_{1-x}$ (see figure 2(a)). This is in contrast to the lattice parameter c, which within the same range is marginally smaller for $^{54}FeSe_{1-x}$ than for $^{56}FeSe_{1-x}$ (figure 2(b)). The lattice volume remains, however, unchanged. Consequently, substitution of ^{56}Fe by ^{54}Fe leads to a small but detectable *enhancement* of the lattice along the crystallographic a and b directions and a *compression* of it along the c-axis, resulting in a change to the shape of the Fe_4Se pyramid, which is known to influence T_c in Fe-based HTS [17]–[19]. This is shown in figure 2(c), where below 100 K the Se atom is located closer to the Fe plane in $^{54}FeSe_{1-x}$ than in $^{56}FeSe_{1-x}$. The corresponding change to the Fe_4Se pyramid is shown schematically in the inset of figure 2(c). It is important to note that the observed Fe-IEs on the lattice parameters are intrinsic and not just a consequence of slightly different samples. As shown in [7], various samples of $^{56}FeSe_{1-x}$ with $1 - x \simeq 0.98$ and $T_c \simeq 8.2$ K indeed exhibit the same lattice parameters within experimental error.

The Fe-IE on the transition temperature T_c was studied by means of magnetization experiments. Measurements were performed by using a SQUID magnetometer (Quantum Design MPMS-7) in a field of $\mu_0 H = 0.1$ mT for temperatures ranging from 2 to 20 K. In order to avoid artifacts and systematic errors in the determination of the isotope shift of T_c, it is

Table 1. Structural parameters of $^{54}FeSe_{1-x}$ and $^{56}FeSe_{1-x}$ at $T = 250$ and 5 K. Space group $P4/nmm$ (no. 129), origin choice 2: Fe in ($2b$) position (1/4, 3/4, 1/2) and Se in ($2c$) position (1/4, 1/4, z). Space group $Cmma$ (no. 67): Fe in ($4b$) position (1/4, 0, 1/2), Se in ($4g$) position (0, 3/4, z). The atomic displacement parameters (B) for Fe and Se were constrained to be the same. The Bragg R factor is given for the main phase; the other reliability factors are given for the whole refinement.

	$T = 250$ K		$T = 5$ K	
	$^{54}FeSe_{1-x}$	$^{56}FeSe_{1-x}$	$^{54}FeSe_{1-x}$	$^{56}FeSe_{1-x}$
Space group	$P4/nmm$		$Cmma$	
Se content	0.975(5)	0.975(4)	Fixed to 0.975	
a(Å)	3.770 36(3)	3.769 88(5)	5.335 23(10)	5.334 26(10)
b(Å)			5.309 84(10)	5.309 33(10)
c(Å)	5.516 19(9)	5.516 37(9)	5.486 83(9)	5.487 87(9)
Volume (Å^3)	156.883(3)	156.797(3)	155.438(5)	155.424(5)
z−Se	0.2319(2)	0.2326(0.3)	0.2321(2)	0.2322(3)
B(Å^2)	1.02(2)	0.93(2)	0.44(2)	0.36(2)
R_{Bragg}	3.11	2.93	4.13	3.63
R_{wp}	3.93	3.72	5.16	4.62
R_{exp}	3.13	3.05	4.73	4.03
χ^2	1.58	1.49	1.19	1.32

important to perform a *statistical* study: i.e. to investigate the series of $^{54}FeSe_{1-x}/^{56}FeSe_{1-x}$ samples synthesized in exactly the same way (the same thermal history and the same amount of Se in the initial composition). The magnetization experiments were conducted for six $^{54}FeSe_{1-x}$ and seven $^{56}FeSe_{1-x}$ samples, respectively. The inset in figure 3 shows an example of zero-field cooled (ZFC) magnetization curves for a pair of $^{54}FeSe_{1-x}/^{56}FeSe_{1-x}$ samples (M_{norm} was obtained after subtracting the small constant paramagnetic offset M_{magn} measured at $T > T_c$ and further normalization of the obtained curve to the value at $T = 2$ K as $M_{norm} = [M(T) - M_{magn}]/[M(2K) + M_{magn}]$, see also figure 1 in [7] for details). The amount of magnetic impurities responsible for the paramagnetic offset at $T > T_c$ is rather small, which is also confirmed by the small value of the ratio $M_{magn}/M(2K)$ corresponding to $\simeq -0.019$ and -0.023 for the particular $^{54}FeSe_{1-x}$ and $^{56}FeSe_{1-x}$ samples shown in the inset of figure 3. The magnetization curve for $^{54}FeSe_{1-x}$ is shifted almost parallel to higher temperature, implying that T_c of $^{54}FeSe_{1-x}$ is higher than that of $^{56}FeSe_{1-x}$. The resulting transition temperatures determined from the intercept of the linearly extrapolated $M_{norm}(T)$ curves with the $M = 0$ line for all samples investigated are summarized in figure 3. The T_cs for both sets of $^{54}FeSe_{1-x}/^{56}FeSe_{1-x}$ samples fall into two distinct regions: $8.39 \leqslant {}^{54}T_c \leqslant 8.48$ K and $8.15 \leqslant {}^{56}T_c \leqslant 8.31$ K, respectively. The corresponding mean values are $^{54}\overline{T}_c = 8.43(3)$ K and $^{56}\overline{T}_c = 8.21(4)$ K. Note that one out of the seven $^{56}FeSe_{1-x}$ samples had $T_c \simeq 8.44$ K, which is by more than 5 standard deviations above the average calculated for the rest of the six samples. We have no explanation for this discrepancy, but decided to show this point for completeness of the data collected.

The Fe-IE exponent α_{Fe} was determined from the data presented in figure 3 using equation (1), where the relative Fe isotope shift of the quantity X is defined as

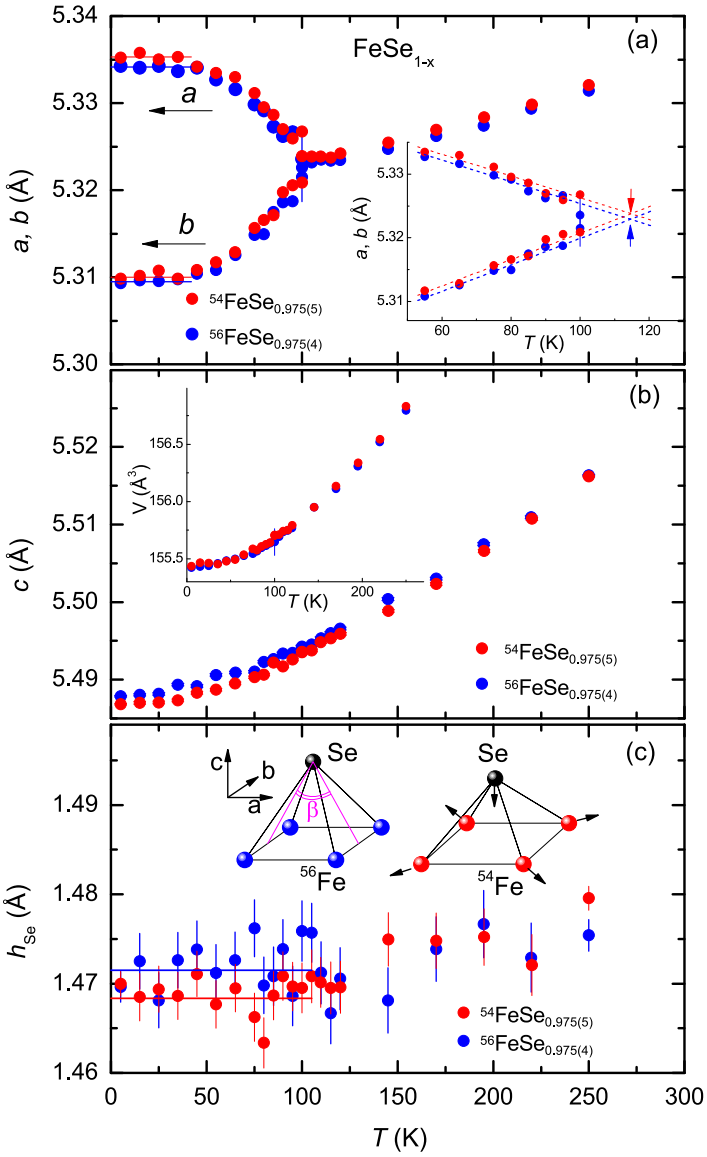

Figure 2. The temperature dependence of the lattice constants a and b (panel (a), in the tetragonal phase a is multiplied by $\sqrt{2}$), lattice constant c (panel (b)) and the distance between the Se atom and Fe plane h_{Se} (panel (c)) for $^{54}\mathrm{FeSe}_{0.975(5)}$ and $^{56}\mathrm{FeSe}_{0.975(4)}$ samples. The inset in panel (a) shows the extended part of $a(T)$ and $b(T)$ in the vicinity of the structural transition temperature T_{s}, together with the linear fits. The inset in panel (b) represents the temperature dependence of the lattice volume V. The inset in panel (c) shows schematically the modification of the Fe_4Se pyramid caused by $^{56}Fe/^{54}Fe$ isotope substitution. The arrows show the direction of atom displacements (see text for details).

$\Delta X/X = ({}^{54}X - {}^{56}X)/{}^{56}X$ (this definition of $\Delta X/X$ is used throughout the paper). With ${}^{54}\overline{T}_{\mathrm{c}} = 8.43(3)$ K, ${}^{56}\overline{T}_{\mathrm{c}} = 8.21(4)$ K, $M_{^{54}\mathrm{Fe}} = 54\,\mathrm{g\,mol^{-1}}$ and $M_{^{56}\mathrm{Fe}} = 55.85\,\mathrm{g\,mol^{-1}}$, one obtains $\alpha_{\mathrm{Fe}} = 0.81(15)$. Three points should be emphasized: (i) the *positive* sign of the Fe-IE exponent α_{Fe} is similar to that observed in phonon-mediated superconductors, such as elemental metals [1]

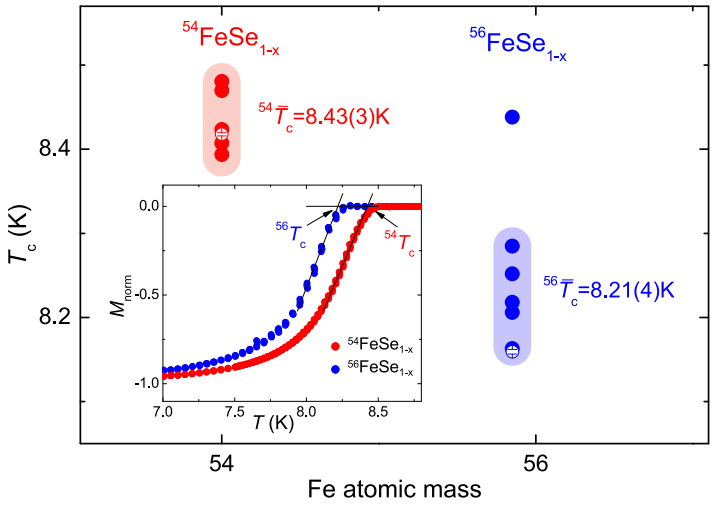

Figure 3. The superconducting transition temperature T_c as a function of Fe atomic mass for $^{54}FeSe_{1-x}/^{56}FeSe_{1-x}$ samples studied in the present work. The open symbols correspond to the samples studied by NPD experiments. The T_cs fall into the regions marked by the colored stripes with the corresponding mean values $^{54}\overline{T}_c = 8.43(3)$ K and $^{56}\overline{T}_c = 8.21(4)$ K. The inset shows the normalized ZFC magnetization curves $M_{norm} = [M(T) - M_{magn}]/[M(2K) + M_{magn}]$ for one pair of $^{54}FeSe_{1-x}$ and $^{56}FeSe_{1-x}$ samples. The transition temperature T_c is determined as the intersection of the linearly extrapolated $M_{norm}(T)$ curve in the vicinity of T_c with the $M = 0$ line.

and MgB_2 [20], as well as in cuprate HTS [21, 22], where the pairing mechanism is still under debate. Bearing in mind that a positive Fe-IE exponent was also observed in $SmFeAsO_{0.85}F_{0.15}$ and $Ba_{0.6}K_{0.4}Fe_2As_2$ [2], we may conclude that, at least for three compounds representing different families of Fe-based HTS (1111, 122 and 11), the sign of the Fe-IE on T_c is conventional. This suggests that the lattice plays an essential role in the pairing mechanism in the Fe-based HTS. (ii) The Fe-IE exponent $\alpha_{Fe} = 0.81(15)$ is larger than the BCS value $\alpha^{BCS} = 0.5$ as well as more than twice as large as $\alpha_{Fe} \simeq 0.35$ reported for $SmFeAsO_{0.85}F_{0.15}$ and $Ba_{0.6}K_{0.4}Fe_2As_2$ [2]. Note that an enhanced value of the oxygen isotope exponent ($\alpha_O \simeq 1$) was also observed in underdoped cuprate HTS [22] and was shown to be a consequence of the polaronic nature of the supercarriers in that class of materials [23]. Recently, Bussmann-Holder *et al* [24] showed that, in the framework of a two-band model, polaronic coupling in the larger gap channel and in the interband interaction induces a T_c (doping)-dependent Fe-IE: α_{Fe} increases strongly with reduced T_c (doping), reaching $\alpha_{Fe} \simeq 0.9$ at $T_c \simeq 10$ K. Note that a similar generic trend is observed in cuprate HTS [21, 22]. (iii) The positive value of the Fe isotope exponent observed in the present study contradicts the results of Shirage *et al* [4], reporting $\alpha_{Fe} \simeq -0.18$ for $Ba_{1-x}K_xFe_2As_2$. As will be shown later, such a difference could arise from the substantial 'structural' contribution to the isotope exponent, which may also allow us to explain the conflicting results of [2] and [4].

Our structural refined NPD data suggest that part of the large Fe-IE $\alpha_{Fe} = 0.81(15)$ may result from the tiny structural changes due to $^{54}Fe/^{56}Fe$ substitution. In the following, we discuss a possible structural effect on the observed Fe-IE on T_c. It is known that in $FeSe_{1-x}$ a decrease

in the Se height caused by compression of the Fe_4Se pyramid leads to an increase in T_c by $\Delta T_c^{h_{Se}}/(\Delta h_{Se}/h_{Se}) \simeq 3.4\,K/\%$ [19, 25]. In contrast, an increase in the Se(Te)–Fe–Se(Te) angle in the $FeSe_{1-y}Te_y$ family (angle β in our notation[6], see the inset of figure 2(c)) results for $y \leqslant 0.5$ in a decrease in T_c by $\Delta T_c^{\beta}/(\Delta\beta/\beta) \simeq 2.9\,K/\%$ [18]. Based on the structural data presented in figure 2, one obtains $\Delta h_{Se}/h_{Se} = 0.22(8)\%$ and $\Delta\beta/\beta = -0.13(4)\%$, leading to $\Delta T_c^{h_{Se}} = 0.7(3)\,K$ and $\Delta T_c^{\beta} = -0.4(2)\,K$ (in this estimate, the values of the lattice constants a and b and h_{Se} were averaged over the temperature regions denoted as solid lines in figures 2(a) and (c)). Bearing in mind that all Fe-based HTS are similarly sensitive to structural changes as $FeSe_{1-x}$ (see, e.g., [17]–[19], [26]), we conclude that the shift in T_c caused by tiny modifications of the crystal structure upon isotope exchange may contribute to the total Fe-IE exponent. However, the large errors of $\Delta T_c^{h_{Se}}$ and ΔT_c^{β} do not allow a reliable estimate of this structural effect on the Fe-IE on T_c. A better estimate of this effect can be made based on the empirical relation between T_c and the lattice parameter a for the 11 family $FeSe_{1-y}Te_y$ [18, 26]. Assuming that the relation $T_c(a)$ is also valid for $FeSe_{1-x}$, one obtains from the data presented in [26] for $y \leqslant 0.5$ the relation $\Delta T_c^{a}/(\Delta a/a) \approx 6\,K/\%$. With $(\Delta a + \Delta b)/(a+b) = 0.0195(14)\%$, this gives rise to a *structural* shift in T_c of $\Delta T_c^{str} \approx 0.1\,K$ (the lattice constants a and b were averaged over the temperature regions marked by a solid line in figure 2(a)). Taking this correction into account yields a rough estimate of the intrinsic Fe-IE exponent of $\alpha_{Fe}^{int} \approx 0.4$. This value is comparable to $\alpha_{Fe} \simeq 0.35$ reported for $SmFeAsO_{0.85}F_{0.15}$ and $Ba_{0.6}K_{0.4}Fe_2As_2$ [2].

To summarize, the $^{56}Fe/^{54}Fe$ isotope effects on the superconducting transition temperature and the crystal structure were studied in the iron chalcogenide superconductor $FeSe_{1-x}$. The following results were obtained: (i) the substitution of the natural Fe ($M_{Fe} = 55.85\,g\,mol^{-1}$) by the ^{54}Fe isotope ($M_{^{54}Fe} = 54.0\,g\,mol^{-1}$) gives rise to a pronounced Fe isotope shift in the transitions temperature T_c as determined by magnetization measurements. The average T_c is found to be $\simeq 0.22\,K$ higher for the $^{54}FeSe_{1-x}$ samples, as compared to the $^{56}FeSe_{1-x}$ samples, resulting in an Fe-IE exponent of $\alpha_{Fe} = 0.81(15)$. (ii) The $^{56}Fe/^{54}Fe$ isotope substitution leads to an enhancement of the lattice constants a and b and a shrinkage of the lattice constant c. These modifications do not affect the lattice volume. (iii) The tetragonal to orthorhombic structural transition temperature ($T_s \simeq 100\,K$) is the same for both $^{54}FeSe_{1-x}$ and $^{56}FeSe_{1-x}$ within the accuracy of the experiment. (iv) For temperatures below 100 K, the distance between the Se atom and Fe plane (Se height) is smaller for the samples with ^{54}Fe. This, together with the results of point (ii), imply that $^{56}Fe/^{54}Fe$ isotope substitution leads to a compression of the Fe_4Se pyramid along the crystallographic c-axis and an enhancement along the a- and b-directions. (v) The structural changes caused by $^{56}Fe/^{54}Fe$ isotope substitution induce a shift in T_c, which may reduce the value of the Fe-IE exponent to ≈ 0.4, in fair agreement with $\alpha_{Fe} \simeq 0.35$ obtained for $SmFeAsO_{0.85}F_{0.15}$ and $Ba_{0.6}K_{0.4}Fe_2As_2$ [2].

In conclusion, from magnetization experiments the Fe-IE exponent of T_c for the $FeSe_{1-x}$ system was determined to be $\alpha_{Fe} = 0.81(15)$. The tiny changes to the structural parameters caused by isotope substitution may contribute to the total Fe-IE exponent, and may help us to clarify, or even be the origin of, the previously reported controversial results [2, 4]. However, more detailed and systematic structural investigations of Fe isotope substituted samples are required in order to draw definite conclusions. Our findings, on the other hand, clearly show that a conventional isotope effect on T_c is present, which highlights the role of the lattice in the pairing mechanism in this new material class.

[6] In the orthorombic phase there are two angles β_1 and β_2, which are different by $\simeq 0.3^\circ$ at $T = 5\,K$.

Acknowledgments

We thank A Bussmann-Holder for fruitful discussions and a critical reading of the manuscript. This work was partly performed at SINQ (Paul Scherrer Institute, Switzerland). The work of MB was supported by the Swiss National Science Foundation. The work of EP was supported by the NCCR program MaNEP.

References

[1] Maxwell E 1950 *Phys. Rev.* **78** 477
Reynolds C A, Serin B, Wright W H and Nesbitt L B 1950 *Phys. Rev.* **78** 487
[2] Liu R H *et al* 2009 *Nature* **459** 64
[3] Carbotte J P 1990 *Rev. Mod. Phys.* **62** 1027
[4] Shirage P M, Kihou K, Miyazawa K, Lee C-H, Kito H, Eisaki H, Yanagisawa T, Tanaka Y and Iyo A 2009 *Phys. Rev. Lett.* **103** 257003
[5] Hsu F C *et al* 2008 *Proc. Natl Acad. Sci. USA* **105** 14262
[6] Khasanov R *et al* 2008 *Phys. Rev.* B **78** 2250510(R)
[7] Pomjakushina E, Conder K, Pomjakushin V, Bendele M and Khasanov R 2009 *Phys. Rev.* B **80** 024517
[8] McQueen T M *et al* 2009 *Phys. Rev.* B **79** 014522
[9] McQueen T M, Williams A J, Stephens P W, Tao J, Zhu Y, Ksenofontov V, Casper F, Felser C and Cava R J 2009 *Phys. Rev. Lett.* **103** 057002
[10] Bendele M, Amato A, Conder K, Elender M, Keller H, Klauss H-H, Luetkens H, Pomjakushina E, Raselli A and Khasanov R 2010 *Phys. Rev. Lett.* **104** 087003
[11] Khasanov R, Bendele M, Amato A, Conder K, Keller H, Klauss H-H, Luetkens H and Pomjakushina E 2010 *Phys. Rev. Lett.* **104** 087004
[12] Fischer P 2000 *Physica* B **276–278** 146
[13] Rodríguez-Carvajal J 1993 *Physica* B **192** 55
[14] Okamoto H 1991 *J. Phase Equilib.* **12** 383
[15] http://www.ncnr.nist.gov/resources/n-lengths
[16] Margadonna S, Takabayashi Y, McDonald M T, Kasperkiewicz K, Mizuguchi Y, Takano Y, Fitch A N, Suard E and Prassides K 2008 *Chem. Commun. (Camb.)* 5607
[17] Zhao J *et al* 2008 *Nature Materials* **7** 953
[18] Horigane K, Hiraka H and Ohoyama K 2009 *J. Phys. Soc. Japan* **78** 074718
[19] Mizuguchi Y, Hara Y, Deguchi K, Tsuda S, Yamaguchi T, Takeda K, Kotegawa H, Tou H and Takano Y 2010 *Supercond. Sci. Technol.* **23** 054013
[20] Budko S L, Lapertot G, Petrovic C, Cunningham C E, Anderson N and Canfield P C 2001 *Phys. Rev. Lett.* **86** 1877
Hinks D G, Claus H and Jorgensen J D 2001 *Nature* **411** 457
[21] Batlogg B, Kourouklis G, Weber W, Cava R J, Jayaraman A, White A E, Short K T, Rupp L W and Rietman E A 1987 *Phys. Rev. Lett.* **59** 912
Franck J P, Jung J, Mohamed M A-K, Gygax S and Sproule G I 1991 *Phys. Rev.* B **44** 5318
[22] Khasanov R, Shengelaya A, Di Castro D, Morenzoni E, Maisuradze A, Savic I M, Conder K, Pomjakushina E, Bussmann-Holder A and Keller H 2008 *Phys. Rev. Lett.* **101** 077001
[23] Bussmann-Holder A and Keller H 2005 *Eur. Phys. J.* B **44** 487
[24] Bussmann-Holder A, Simon A, Keller H and Bishop A R 2010 *J. Supercond. Nov. Magn.* **23** 365
Bussmann-Holder A, Simon A, Keller H and Bishop A R 2009 arXiv:0906.2283
[25] Margadonna S, Takabayashi Y, Ohishi Y, Mizuguchi Y, Takano Y, Kagayama T, Nakagawa T, Takata M and Prassides K 2009 *Phys. Rev.* B **80** 064506
[26] Mizuguchi Y, Tomioka F, Tsuda S, Yamaguchi T and Takano Y 2009 *J. Phys. Soc. Japan* **78** 074712